Histological Imaging of Unstained Cancer Tissue Samples by Circularly Polarized Light

Viktor Dremin[1,2], Oleksii Sieryi[3], Mariia Borovkova[3], Juha Näpänkangas[4], Igor Meglinski[1,3], and Alexander Bykov[3*]

[1]*College of Engineering and Physical Sciences, Aston University, B4 7ET Birmingham, UK*
[2]*Research & Development Center of Biomedical Photonics, Orel State University, 302026 Orel, Russia*
[3]*Optoelectronics and Measurement Techniques Unit, University of Oulu, 90014 Oulu, Finland*
[4]*Department of Pathology, Oulu University Hospital, 90220 Oulu, Finland*
** Correspondence: alexander.bykov@.oulu.fi*

Abstract: We introduce a high-resolution polarization imaging approach for automatic stand-alone classification of the unstained breast cancer tissue blocks by using K-means cluster analysis of the Stokes vectors projected on the Poincaré sphere.

1. Introduction

The current practice of microscopic histological examination of cancer samples includes routine and time-consuming preparation steps such as tissue slicing, staining, and manual inspection. The instant availability of high-quality histopathological images supported by the automated analysis could substantially improve the efficacy and reliability of the diagnostic procedures. In many cases, cancer is associated with the microstructural changes of biotissues such as cell nucleus enlargement [1], general structural reorganization, etc. The high sensitivity of the circularly polarized light to the subtle variations in the tissue structure [2] makes it a promising tool for the detection and staging of cancer [3-5]. In this study, we suggest using the circularly polarized light for the non-destructive analysis of formalin-fixed paraffin-embedded (FFPE) breast cancer samples. In particular, we propose point-by-point measurements of the full Stokes vector of the diffusely reflected light and the automated segmentation of the obtained images by the *k*-means cluster analysis of the Stokes vectors of the detected light.

2. Materials and methods

The imaging setup consists of the illumination and detection channels as well as a precision XY stage allowing the spatial sample scanning in the lateral dimensions. The schematics of the setup is presented in Fig. 1. In the illumination channel, the light of the supercontinuum fiber laser (Leukos Ltd., France) has been guided through the acousto-optic tunable filter (Leukos Ltd., France) enabling the selection of the probing wavelength in the range of 450-650 nm. The linearly polarized light from the output of the filter has been turned to the state of the right circular polarization with the quarter-waveplate and focused onto the sample surface with the 45 mm lens. The use of circular polarization allows the light to preserve its polarization properties during a larger number of scattering events than linear polarization.

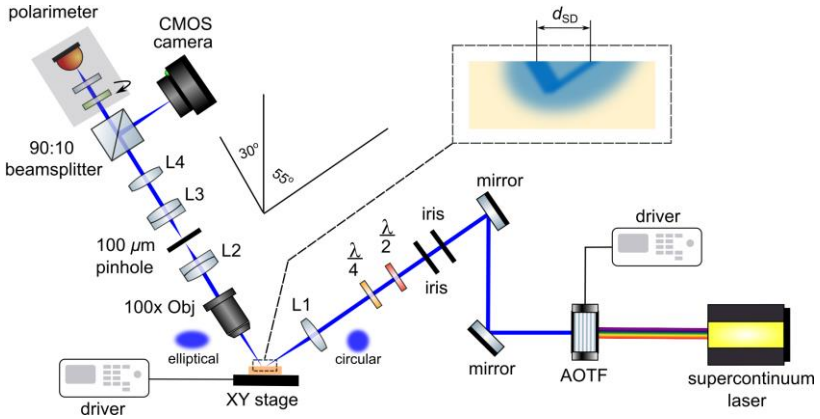

Fig. 1. Schematics of the polarization imaging setup. The illumination arm (right side) delivers the circularly polarized light onto the sample. The detection arm (left side) performs the point measurements of the Stokes vector of the diffusely reflected radiation. Precise spatial scanning of the sample is carried out with the translation XY stage.

The diffusely reflected polarized light was collected with the 100× objective at a variable distance d_{SD} from the point of the incidence. The collected light was then spatially filtered with a 100 μm pinhole to reject the out-of-focus signal. The combination of the objective and the pinhole used provides the field of view with a diameter of 10 μm. A polarization state analysis of the reflected light has been performed with the Stokes polarimeter (Thorlabs Ltd., USA). 90:10 beam-splitter was used to split the optical signal between the polarimeter and CMOS camera used to control the focus position of the objective on the sample's surface. Spatial scanning of the sample was performed with a step of 0.5 or 5 μm, depending on the size of the area of interest. The experimentally determined spatial resolution of the system was better than 5 μm.

Unstained FFPE tissue block containing the samples of early-stage breast cancer (ductal carcinoma *in situ*, DCIS) has been used for the measurement. Prior to the measurements, the adjacent slice of the tissue from the block has been characterized by standard histopathological analysis. Fig. 2a shows the conventional histological image of the area of interest provided by the certified pathologist. The considered zone is represented by three tissue types: surrounding fat tissue, benign fibrosis, and epithelial cancerous tissues located inside the milk duct.

3. Results and conclusions

Multiple measurements of the selected region have been performed to find the most optimal scanning parameters of the setup. It was found that the best image contrast is achieved for the wavelength of 450 nm. The optimal source-detector distance d_{SD} was found to be in the range of 60-100 μm. The lower distances result in the decrease of the sensitivity to the presence of the cancerous cells and increase the sensitivity to the surface defects. The increase of the source-detector space over the mentioned range leads to the more substantial depolarization of the light, loss of the polarization signal, and intense noise in the measurements.

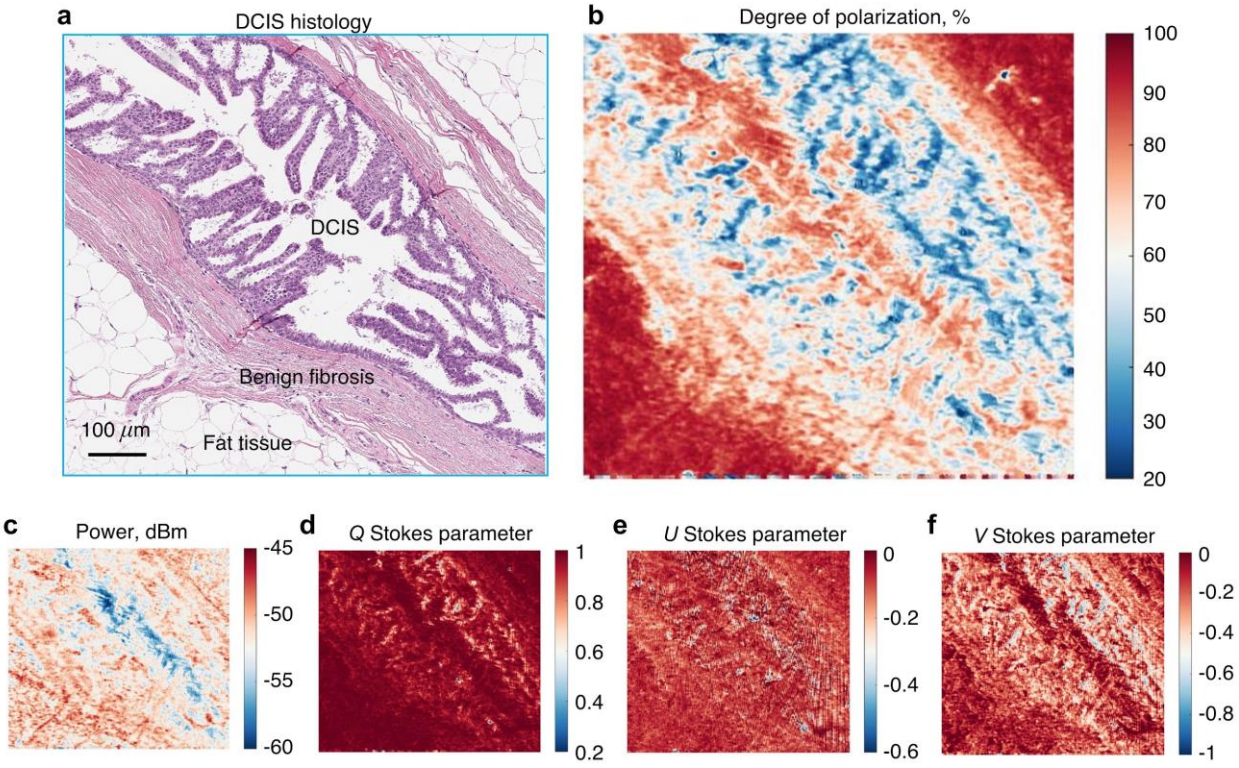

Fig. 2. (a) Histological image of DCIS sample; (b) DOP map of the reflected radiation in the area of interest. 2D spatial distributions of the measured Stokes vector: (c) power, (d) *Q*, (e) *U*, and (f) *V* components.

The spatial maps (2D distributions) of four components of the Stokes vector (power, *Q*, *U*, *V*) measured across the selected region at the optimized setup parameters are presented in Fig. 2c-f. The calculated DOP is shown in Fig. 2b. It was found that the DOP is the most sensitive parameter indicating the malignancy of the tumor. For the intact adipose tissue, the DOP was at the level of 90% or higher, for fibrosis – 65-75%, for DCIS – 45-55%. It is worth noting that the map of the first Stokes vector component (Fig. 2c) representing the scalar intensity does not show a significant correlation with the histological image due to the insensitivity of that parameter to the structural changes

in the tissue. It is also seen from the *V* Stokes component map that the cancerous regions have lower *V* values than the surrounding tissues that can be explained by the increased scattering anisotropy in that regions due to the increase in the size of the scatterers [3].

The obtained measurement data has been depicted on the Poincaré sphere to highlight the changes in the polarization caused by the interaction with the tissue (see Fig. 3a). Cluster analysis based on the *k*-means algorithm using the Euclidean distance metric has been performed to implement the automated classification of the obtained data and delineate cancer zones of the FFPE specimens (Fig. 3b). In this study, the values of *Q, U,* and *V* parameters were used as input information for clustering. Three clusters were used.

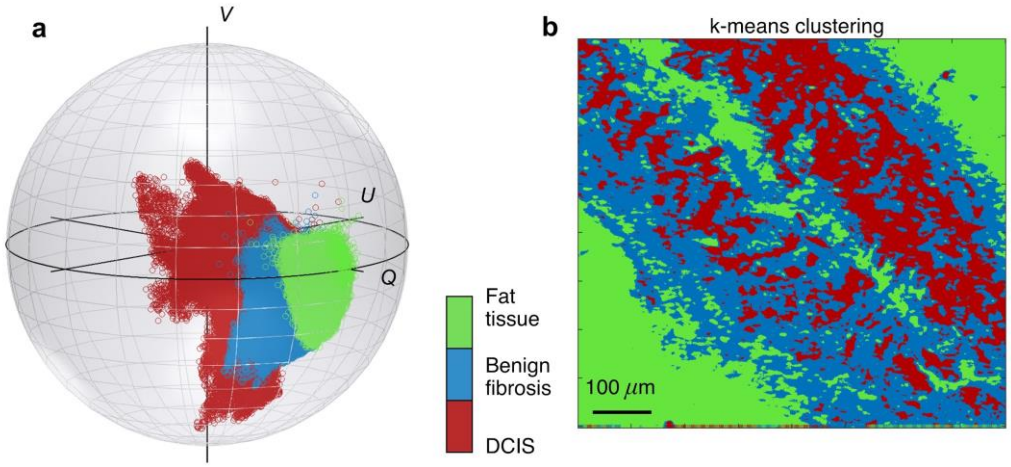

Fig. 3. (a) Clustering results in Poincaré sphere space: green markers – fat tissue, blue – benign fibrosis, red – DCIS; (b) corresponding segmentation based on *k*-means clustering calculated from a full *Q, U, V*-dataset.

Thus, the automated stand-alone segmentation highlights the main regions of the tissue block that are in good agreement with the ground truth provided by standard pathological analysis. The cancerous cells are shown located inside the duct surrounded by the fibrotic and fat tissue. The proposed methodology demonstrates a high potential to revolutionize routine procedures currently used in histological tests in day-to-day clinical practice.

4. Acknowledgements

This work was supported by the Academy of Finland (grants 314369 and 325097), the ATTRACT project funded by the EC under Grant Agreement 777222; and in part by the INFOTECH strategic fund. VD kindly acknowledges personal support from the Russian Science Foundation (project No. 19-79-00082, experimental data processing). Authors acknowledge Northern Finland Biobank Borealis, Oulu, Finland (www.ppshp./biopankki) for providing the breast cancer samples.

5. References

[1]. K. Dahl, A. Ribeiro, and J. Lammerding, "Nuclear shape, mechanics, and mechanotransduction," Circ. Res. **102**, 1307-1318 (2008).

[2] N.G. Khlebtsov, I.L. Maksimova, I. Meglinski, V.V. Tuchin, and L.V. Wang, "Introduction to Light Scattering by Biological Objects: Extinction and Scattering of Light in Disperse Systems", in: *Handbook of Optical Biomedical Diagnostics*, Ed. V. Tuchin, SPIE Press, Chapter 1 (2016).

[3] B. Kunnen, C. Macdonald, A. Doronin, S. Jacques, M. Eccles, and I. Meglinski, "Application of circularly polarized light for non-invasive diagnosis of cancerous tissues and turbid tissue-like scattering media," J. Biophotonics **8**, 317-323 (2015).

[4] D. Ivanov, V. Dremin, A. Bykov, E. Borisova, T. Genova, A. Popov, R. Ossikovski, T. Novikova, and I. Meglinski, "Colon cancer detection by using Poincaré sphere and 2D polarimetric mapping of *ex vivo* colon samples," J. Biophotonics **13**, e202000082 (2020).

[5] V. Dremin, D. Anin, O. Sieryi, M. Borovkova, J. Näpänkangas, I. Meglinski, and A. Bykov, "Imaging of early-stage breast cancer with circularly polarized light," Proc. SPIE **11363**, 1136304 (2020).